γ→α' Martensitic Transformation in the Reactor Steels Under Irradiation and Deformation

Darya ALONTSEVA [1 *], Oleg MAKSIMKIN [2], Alyona RUSSAKOVA [2,3], Sergey SUSLOV [4]

[1] *East-Kazakhstan State Technical University, Ust-Kamenogorsk, 69 Protazanov St., 070004, Kazakhstan*
[2] *Institute of Nuclear Physics NNC RK, Almaty, 1 Ibragimov, 050032, Kazakhstan*
[3] *L.M. Gumilev Eurasian National University, Astana, 5 Munaitpasov St., 010008, Kazakhstan*
[4] *School of Materials Engineering, Purdue University, West Lafayette, IN 47906, USA*

crossref http://dx.doi.org/10.5755/j01.ms.20.1.1904

Received 17 June 2012; accepted 06 January 2013

Complex studies of the 12Cr18Ni10Ti and Cr15Mn14 reactor steels in the initial, deformed states, and after irradiation with the $^{84}_{36}Kr^{+14}$ and WC^{+} heavy ions were conducted. Peculiarities of the α'-martensite phase content and mechanical characteristics of the specimens, which were deformed after the irradiation were examined. It was shown that the martensite phase existed in the irradiated and deformed specimen at two scale levels. Electron Backscattered Diffraction (EBSD) revealed that the difference between the unirradiated and irradiated specimens was the formation of the α'-martensite and ε-martensite in the near surface layer of the irradiated specimen. It was determined that the fluence value has affect on the α'-magnetic phase. Thus, chrome-nickel steels of 12Cr18Ni10Ti type show better resistance to irradiation with the heavy WC^{+} ions in comparison with manganese steel of Cr15Mn14 type, as less martensite of irradiation forms in them.

Keywords: reactor steels, irradiation, heavy ions, deformation, martensitic transformation.

1. INTRODUCTION

In connection with the development of thermonuclear technology the topical character of the problem of the selection of materials for the nuclear reactor first wall and the diverter device rises. These materials must be capable of preserving mechanical properties under the critical conditions of repeated irradiation with the flows of accelerated particles in a wide range of energy and mass and at significant drops in temperature and stress for a long time. Austenitic stainless steels, widely used in the reactor engineering, are considered promising construction materials for the projected thermonuclear installations. At the same time, along with the chrome-nickel steels, the manganese steels are considered promising because they do not contain nickel and therefore become slightly radioactive after irradiation.

It is known that under the conditions of external loading and radiation damage austenitic stainless steels reveal a change in the phase-structural state, related to the formation of the α'-martensite of deformation [1, 2]. The formation of α'-martensite of deformation can substantially influence the strength, plastic and magnetic properties of the materials. This is relevant for chrome-nickel steels, and is even more relevant for manganese steels, which are characterized by smaller stacking fault energy and higher tendency toward the formation of martensite [3]. Since the irradiation with accelerated charged particles leads to the formation of the α'-martensite impregnations in the near-surface layers of the steel specimens [4, 5], it was expected that the bombardment with heavy ions even with relatively low energies (several tens of keV) can influence the state of the steel with the already formed α'-phase. Until recently, the diffusionless γ→α' transformation, which takes place during cold working of the stainless steels, was investigated using such methods as Transmission Electron Microscopy (TEM), X-ray diffraction and by the determination of magnetic properties [6]. At the same time, in the latter case, not only the volumetric content of the α'-phase was measured, but also its distribution along the effective length of a specimen. However, from the analysis of the results of these measurements it was unclear what changes in the microstructure were responsible for the increase in the magnetic characteristics. The application of X-ray diffraction analysis for this purpose to a small (up to 2 %–3 %) volume fraction of the ferromagnetic α'-phase is limited by its sensitivity. The use of a method of Transmission Electron Microscopy assumes the destruction of a sample under investigation, which is unacceptable in most cases. In this connection, the study of the dependences of the γ→α' transformation requires more sensitive techniques capable of capturing insignificant changes in the microstructural and phase state of a material and combining them with the data on the elemental composition changes or local orientations of crystallites. EBSD is one of the techniques that can be used. This technique is used to study a variety of crystalline materials and, in particular, for the determination of microtextures, the orientation of crystallites and properties of the grain boundaries [7, 8].

The paper presents the results of the experiments on examining the structural-phase changes in the near-surface layer of austenitic steels, deformed in tension at room temperature and irradiated by the $^{84}_{36}Kr^{+14}$ and WC^{+} high-energy heavy ions.

* Corresponding author. Tel.: +7-7232-252533; fax: +7-7232-267409.
E-mail address: *dalontseva@mail.ru* (D. Alontseva)

2. EXPERIMENTAL DETALS

The objects for this study were two sets of specimens made of 12Cr18Ni10Ti and Cr15Mn14 stainless steels (austenized at 1050 °C, 30 min) subjected to static tension at 20°C. As a result of the deformation, the ferromagnetic α'-phase formation was initialized in the specimens. The steel specimens from the first set, deformed to certain degree (40 % – 50 %), were unloaded while the values of the current load and a change in the magnetometric signal according to the diagram, described in [9] were simultaneously recorded. The working part of the deformed specimens was then evenly irradiated by the 50 keV tungsten carbide ions (WC^+) on the "Diana" accelerator facility up to the fluence of 8.9×10^{18} ions/cm^2. After the irradiation, the specimens were further deformed at tension up to failure. The F 1.05 ferromagnetic probe was used before and after the irradiation to determine the change in the magnetic response along the length of the deformed specimens, which characterized the distribution of the ferromagnetic α'-phase. The presence of the martensite phase was additionally confirmed by the analysis of the microstructure of the deformed specimens using TEM. The specimens were cut from the "neck" area and the TEM employed was JEM-100CX.

The steel specimens of the same composition from the second set were irradiated by the $^{84}_{36}Kr^{+14}$ high-energy ions on the DC-60 accelerator. For the purpose of irradiation, four flat 300 μm thick specimens designed for mechanical tests were mounted in a special holder (Fig. 1) and placed into the vacuum chamber which was then evacuated down to the pressure of 10^{-4} Pa.

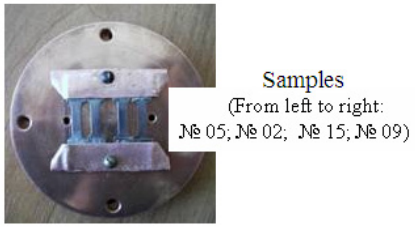

Fig. 1. A copper specimen holder for irradiation of four specimens in the vacuum camera in the DC-60 heavy ion accelerator

The temperature during irradiation was maintained below 100 °C. The target was cooled down by the water cooling system. The irradiation process had two stages. At the first stage, the specimens numbered 02 and 15 were irradiated up to the fluence of 4×10^{15} ions/cm^2 (E = 1.56 MeV/nucleon) while the specimens numbered 05 and 09 were irradiated up to the fluence of 1×10^{15} ions/cm^2. One year later, the same specimens were again irradiated in the same conditions up to the total fluence 9×10^{15} ions/cm^2 for specimens 02 and 15 and up to 6×10^{15} ions/cm^2 for specimens 05 and 09 correspondingly.

The amount of the ferromagnetic phase in the initially paramagnetic steel was determined with the Feritoscope MP-30 ferromagnetic probe with ~0.01 % error. The X-ray diffraction analysis of the phase state of the initial, deformed and irradiated specimens was conducted on the D8 Advance (Bruker AXS GmbH) system using the CoK_α irradiation. The step was 2 deg/min and the sample was rotated at the speed of 60 r/min, which allowed obtaining more complete information on the diffracting planes from different phases in the steel specimens. The absolute accuracy of the determination of θ and of 2θ angles was ±0.005º. The observation of the irradiated surface of the specimens and phase analysis were carried out in the JSM-7500F SEM (JEOL, Japan). The EBSD system also installed on this microscope was used to obtain the microtexture information via the analysis of the Kikuchi diffraction patterns with the application of diffraction data database. In this method, the lateral resolution was 200 nm and the angular resolution was 1º. The step of the automatic determination of the orientation on the surface was 0.05 μm. The area scanned and analyzed in each experiment was (310×230) μm. The experiment total scan time was about 4 h.

Briefly, the method of EBSD analysis consists in the following. The polished specimen, inclined at a 70° angle, is placed into the scanning electron microscope and the surface being examined undergoes the automatic step-by-step scanning "from one point to the next". The most difficult part in the EBSD method is the preparation of the surface of a specimen. The high requirements for the surface roughness are in view of the fact that the specimen during scanning is inclined at a significant angle and even relatively small relief can substantially affect the results, e. g. reduce "the degree of the recognizability" of one phase or another. For the steel specimens examined, this value of "recognizability" was at 60 % – 85 %. It should be noted that "recognizability" is automatically adjusted by the program up to 100 %.

3. RESULTS AND DISCUSSION

3.1. Martensitic γ→α′ transformation during deformation

Fig. 2, a, shows the characteristic microstructure of the deformed stainless steel. Slips lines, twins and separate plates of the α′-martensite phase can be seen.

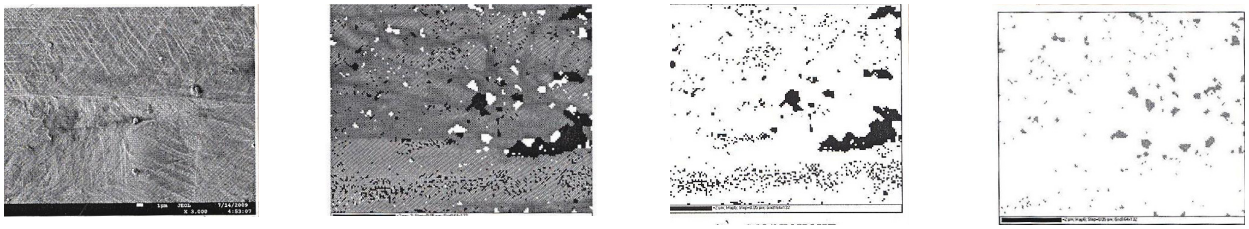

a | b austenite | c α′-martensite | d ε-martensite

Fig. 2. Typical relief on the surface of the 12Cr18Ni10Ti steel specimen deformed in tension at 20 ºC (a); EBSD phase maps for the deformed steel specimen (b, c, d)

The same information can be obtained from the EBSD phase distribution maps from the steel specimen (Fig. 2, b, c, d), from which it follows that the material has three phases. There are both ε-phase (HCP) and α′-martensite of deformation present in the austenitic matrix which is confirmed by the magnetometry data, and which does not contradict the previous data [10]. The characteristic size of the α′-martensite of deformation phase is on the order of several micrometers which is also in the agreement with the majority of the published literature. At the same time, the austenitic grains reveal the presence of very finely dispersed particles of α′-martensite (the hundredths of a micron) uniformly distributed in the matrix. In other words, the matrix of the stainless steel specimen has α′-martensite at two levels: micron and sub-micron levels.

3.2. Martensitic γ→α′ transformation during $^{84}_{36}Kr^{+14}$ ion irradiation

Fig. 3 shows images of the surface topography of the steel specimens irradiated with the $^{84}_{36}Kr^{+14}$ ions (E = 1.56 MeV/nucleon) up to different fluence values. It can be seen that after the bombardment with accelerated heavy particles (1×10^{15} ions/cm^2), the irradiated surface reveals the presence of "secondary formations" like carbides, nitrides and blisters – cavities in the near-surface layer filled with gas. The main reason for these features to be identifiable on the surface probably is:

– for carbides and nitrides – accelerated ion etching of austenite compared to harder particles;

– for blisters – "stuck" Kr atoms and their association in the near surface layer.

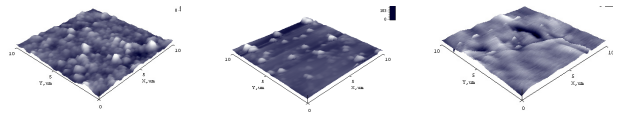

a b c

Fig. 3. Surface topography of the 12Cr18Ni10Ti steel specimen irradiated by $^{84}_{36}Kr^{+14}$ ions (E = 1.56 MeV/nucleon) for several fluencies 1×10^{15} ions/cm^2 (a), 4×10^{15} ions/cm^2 (b), 9×10^{15} ions/cm^2 (c)

The average size of carbide (nitride) particles is 100 nm – 200 nm. The blisters in the images have regular rounded shape unlike carbides (nitrides), and their diameter is much smaller than the size of the "secondary formations" and is of the order of 20 nm – 60 nm. When the dose is increased up to 9×10^{15} ions/sm^2, an intensive formation of open blisters (snowflakes) and erosion of the surface along with the blister formation take place (Figs. 3, 4). The surface elemental analysis performed on the small rounded formations observed inside the crystallites confirmed the assumption that they were carbide particles ($Cr_{23}C_6$ chromium carbides) (Table 1). The analysis of the matrix and secondary formations, (supposedly blisters), is practically identical. When the fluence is increased, titanium carbides along with chromium carbides were observed on the specimen irradiated surface.

Since the irradiation and/or plastic deformation results in the formation of a magnetic phase in the paramagnetic austenite with the lattice parameter different from the lattice parameter of the matrix, the experiments with X-ray diffraction and ferromagnetic probe were used. However, taking into account the fact that the magnetic field of the probe is large (~1 mm) and the sensitivity of the diffractometer does not make it possible to reveal such a low (fraction of a percent) volume fraction of the ferromagnetic phase, its quantity and morphology were determined by the method of EBSD analysis. Fig. 5 shows the images obtained with the EBSD analysis. There can be seen unevenly distributed defects looking like "fish-scale" and inflations. The comparison with Fig. 5, a, where grain structures are depicted reveals that the density of blisters varies in different grains – the defect density in some crystals is relatively low, while in others it is substantially higher.

The phase distribution map shows that as a result of irradiation by high energy heavy particles (α′ and ε) form in the surface layer of the 12Cr18Ni10Ti steel specimen. The special feature of the α′-phase is the extraordinary fine dispersion (less than 100 nm). Besides, the bcc phase is predominantly formed in 'pure regions' where the blisters are absent.

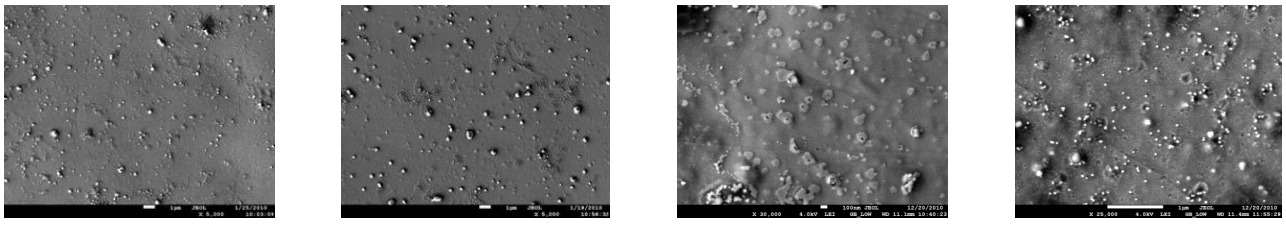

a b c d

Fig. 4. Micrographs of the surface structure of the 12Cr18Ni10Ti steel specimens irradiated by $^{84}_{36}Kr^{+14}$ ions (E = 1.56 MeV/nucleon) for several fluences: 1×10^{15} (a), 4×10^{15} (b), 6×10^{15} (c), 9×10^{15} ions/cm^2 (d)

Table 1. The element analysis of carbide particles

Fluence ions/cm^2	Element	C	Al	O	Si	Ti	Cr	Mn	Fe	Ni	Tot.
1×10^{15}	Content, %	24.2	0.3	–	0.5	0.4	14.2	0.8	51.9	7.4	100
9×10^{15}		18.1	–	2.3	–	2.0	14.5	0.9	54.4	7.42	100

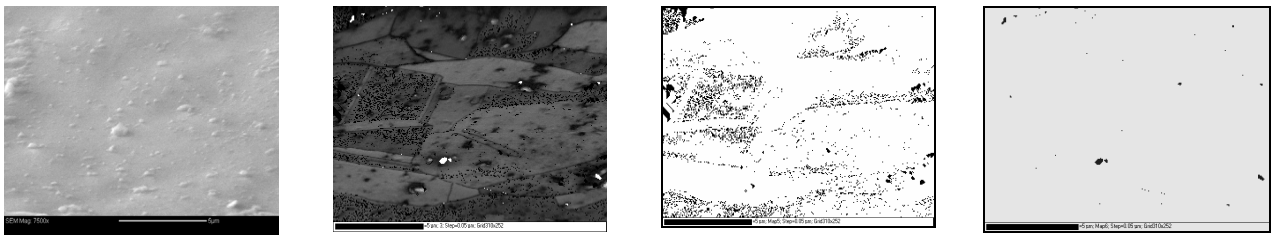

a b c d

austenite α′-martensite ε-martensite

Fig. 5. EBSD phase map obtained from the 12Cr18Ni10Ti steel specimen irradiated by $^{84}_{36}Kr^{+14}$ ions (E = 1.56 MeV/nucleon) up to the fluence of 1×10^{15} ions/cm^2 (50 nm scan step), ×7500

The order distributing feature is that α′-martensite appears in the grains which are predominantly (001) oriented and nucleates mainly at the grain boundaries. At the same time, ε-martensite (hcp) nucleates in the grains which are (111) oriented.

What attracts one's attention is the fact that the orientation of the grain, in which the phase transformation takes place, does not change with the change in the fluence of ions. Fig. 6 also makes it possible to assume that the orientation of a grain is the factor, which determines the form of the defect structure: whether blisters (101), or α′-phase (001) are formed. The amount of the magnetic phase in the steel increases with the ion fluence. For example, in the steel specimen irradiated with the ion fluence of 1×10^{15} ions/cm^2, the α′-phase content is about 8 % (ε-martensite: 1 %); however, in the sample irradiated with the ion fluence of 4×10^{15} ions/cm^2, the α′-phase content is about 9 % (ε-martensite: 2 %).

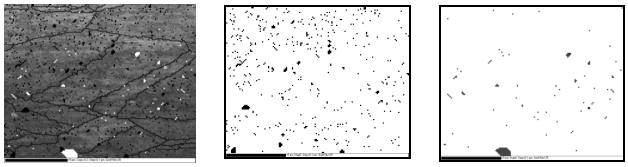

a b c

Austenite α′ – martensite ε – martensite

Fig. 6. EBSD phase map obtained from the 12Cr18Ni10Ti steel specimen irradiated by $^{84}_{36}Kr^{+14}$ ions (E = 1.56 MeV/nucleon) up to the fluence of 6×10^{15} ions/cm^2 (100 nm scan step), ×7500

3.3. Martensitic γ→α′ transformation during deformation and irradiation with heavy ions

The obtained "stress σ – strain δ" curves, and the curves of the change in "M_f – δ" magnetometric signal (which reflect the kinetics of the accumulation of the ferromagnetic α′-martensite in a paramagnetic austenitic matrix being deformed) for the 12Cr18Ni10Ti and Cr15Mn14 steel specimens before and after irradiation with heavy ions are shown in Fig. 7, a, c. The magnetometric measurements data on the ferromagnetic phase content along the working part of the specimens (in the unloaded state) before and after irradiation are shown in Fig. 7, b, d.

Table 2 depicts the values of mechanical and magnetic characteristics calculated on the basis of the diagrams for the specimens before and after irradiation with the WC^+ heavy ions.

Table 2. Mechanical and magnetic characteristics of the steel specimens before and after ion bombardment

Steel	Cr15Mn14	12Cr18Ni10Ti
$\sigma_{0.2}$ before irradiation, N/mm^2	360	210
σ^{M}_{crit} before irradiation, N/mm^2	557	243
δ^{M}_{crit} before irradiation, %	14	20
Typical values of σ_B before irradiation, N/mm^2	800	680
σ_B after irradiation, N/mm^2	790	720
δ after irradiation $^{+}$WC, %	61	59.3
$\Delta M_f^{irr\,1}$, rel.units	0.305	0.095
$\Delta M_f^{irr\,2}$, rel units (under loading)	0.266	0.026
Hardening after irradiation $\Delta\sigma^{irr}$ N/mm^2	64	16.2

The plasticity values for the non-irradiated Cr15Mn14 and 12Cr18Ni10Ti specimens are ~60 % and ~55 % correspondingly. As it follows from Table 2, irradiation of the near-surface layers of the Cr15Mn14 steel specimen which was previously deformed to 48.5 % by heavy ions, practically did not lead to a change in the general plasticity in comparison with the non-irradiated specimen. In the case of 12Cr18Ni10Ti steel specimen (previously deformed to 41.6 %), the plasticity slightly increased (4 %) in comparison with the non-irradiated specimen. Nevertheless, the irradiation changed the phase state of the specimen which showed up as the increase in M_f and additional work hardening (Fig. 7). In the case of the manganese steel, which is more inclined to the formation of α′-martensite of deformation, the irradiation has led to a significant change in the phase state of the specimen which is reflected in the loading curve rising to the abscissa and the level of the flow stresses increasing (for steel 12Cr18Ni10Ti such changes are hardly noticeable). An increase in the σ value (relative to σ_B) after the loading of the irradiated specimens for the second time for steels Cr15Mn14 and 12Cr18Ni10Ti was ~8 % and ~2.3 % correspondingly. The integral increase of ΔM_f^{irr} (for the irradiated and unloaded specimen) made 14 % of the M_f^S value (for unloaded non-irradiated sample) for steel Cr15Mn14 and 33 % – for 12Cr18Ni10Ti.

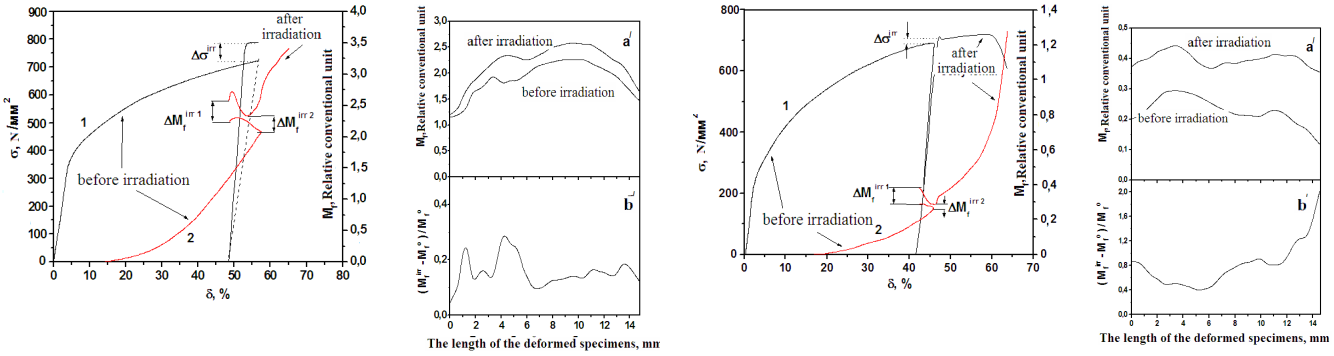

Fig. 7. "Stress σ – strain δ" diagrams (1) and magnetometric curves "M_f – δ" (2) for steel Cr15Mn14 (a) and 12Cr18Ni10Ti (c) specimens before and after irradiation with the WC^+ ions (8.9×10^{18} ions/cm^2). The diagrams of the change of the ferromagnetic phase content along the length of the deformed specimens before and after irradiation (a′); relative increase in the amount of the ferromagnetic phase after irradiation (b′) along the length of the specimens for Cr15Mn14 (b) and 12Cr18Ni10Ti (d)

It should be noted that after irradiation the nature of the curves M_f with unloading and consecutive loading of the steel specimens changes. TEM micrographs showing the microstructure of the deformed specimens cut from the "neck" are illustrated in Fig. 8.

It follows from Fig. 7, b, d, that the contents of the ferromagnetic phase in the near-surface layers after irradiation by heavy ions increases along the working part of the specimen. The increase in ΔM_f can be seen for the areas, which had already contained the martensitic phase before irradiation. It should be noted that in the regions with previously high M_f values before the irradiation, its relative increase after irradiation, generally, is much less than in the boundaries of the working part of the specimen, where M_f becomes several times higher. It is especially noticeable in the case of steel 12Cr18Ni10Ti, for which the maximum relative increase ΔM_f is restricted to the areas with lower initial values of M_f. In the case of steel Cr15Mn14, the local maxima of the ΔM_f increase is found not at the boundary of the working part of the specimen, but at the distance of ~1 mm from it.

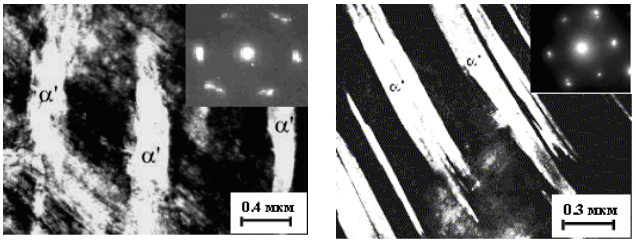

Fig. 8. α′-martensite in the microstructure in the "neck" region for Cr15Mn14 (a) and 12Cr18Ni10Ti (b) specimens after deformation in tension. The insets are diffraction patterns taken at the $[110]_\gamma$ zone axis of the austenitic matrix

On the "M_f –δ" diagrams, the magnetic response from the steel specimen before unloading can be designated as M_f^D which is analogous to M_f^S for the unloaded specimen. These values are combined in the relationship of the form $M_f^S = M_f^D + \Delta M_f$. For the 12Cr18Ni10Ti and Cr15Mn14 steel specimens in the region of the uniform deformation (before irradiation by the WC^+ ions), $M_f^S > M_f^D$ (i. e. $\Delta M_f > 0$). After the irradiation, during the second loading of the specimen, the relationship $M_f^S > M_f^D$ holds in the area of the elastic deformation, and the tensile strength is practically reached as soon as the loading of the specimen starts. As a result of irradiation, the ΔM_f value increases, while the magnetoelastic effect related to the change in the magnetization of the specimens, after external loading is removed and the second loading is applied, is manifested more strongly in steel Cr15Mn14 in comparison with steel 12Cr18Ni10Ti, which is obviously governed by the initially higher content of α′-martensite in the manganese steel. The bombardments of the steel specimens with the 50 keV WC^+ ions lead to local heating and radiation damage of the near-surface layer of the material, but in contrast to the experiments on irradiation of the steels with higher energy ion and electron fluxes discussed in [4, 5] did not result in the γ→α′ transformations at the depth of several micrometers from the surface.

Thus, after irradiation of the undeformed steel specimens by the WC^+ ions, inspection using a ferromagnetic probe did not show any presence of a ferromagnetic phase in them. At the same time, the bombardments with ions of the previously deformed steel specimen lead to a noticeable change in their magnetic properties. Apparently, the main changes in this case occur in a thin near-surface layer, which contains a higher concentration of the martensitic formations in comparison with the bulk; and they are related to the "elastic martensite" (martensite of stress). This term was introduced in [9] for the designation of the unstable part of the α′ phase, whose content can easily change as a result of removal of the load and consecutive loading of plastically deformed steel. The difference between M_f^S and M_f^D and complicated behavior of the $M_f(\delta)$ curve during unloading and consecutive loading can be explained in terms of the magnetoelastic effect and by the presence of the elastic martensite in the steel specimens being deformed. In general, the formation of the bcc-martensite leads to higher stress levels in the surrounding austenitic (fcc) matrix due to the difference in the volumes per one atom in the unit cells, which in turn increases the energy barrier for the γ→α′ transformation and stops further formation of the α′ phase. Partial annealing (relaxation) of the elastic stresses from compression takes place probably due to local

heating in the near-surface layer, and it becomes possible for some micro volumes of the γ phase to be transformed into the α' phase. These micro volumes in the critical, "boundary" state capable of undergoing the direct γ→α' and reverse α'→γ transformations under sufficiently weak external impacts (removal of the load or local heating of the material), display the characteristics of the elastic martensite. If the $M_f(\delta)$ magnetometric curve for the non-irradiated steel is extrapolated to the region of large deformations, then it will eventually intersect (or even coincide with) the $M_f^{irr}(\delta)$ curve for the irradiated steel. The values of the steel magnetic response increased after the irradiation correspond to the beginning of the processes of localization of deformation and formation of a neck in the case of the non-irradiated material. The near-surface layers of specimens, which have higher relative content of the martensitic formations in comparison with the bulk, are strengthened more robustly and the formation of microscopic cracks, which determine the beginning of the process of destruction in them, will apparently start earlier. The hardening in steel Cr15Mn14 is more pronounced in comparison with steel 12Cr18Ni10Ti because of the higher tendency to the formation of the martensite of deformation. It should be noted that the resulting plasticity (i. e. after initial deformation in tension, bombardment with heavy ions and the final deformation in tension till failure) does not practically differ from the case of non-irradiated steel specimens. This indicates that the main contribution to the increase in plasticity of the steel specimens comes from the bulk of the material, which is immune to the strengthening effect of the ion irradiation.

4. CONCLUSIONS

As a result of the irradiation of the stainless steel with heavy ions (E = 1.56 MeV/nucleon) with the fluence of 9×10^{15} ions/cm^2, the TEM data reaveled the formation of the so called "α'-martensite of irradiation" and ε-phase in the near-surface layer, without additional deformation. It was determined by EBSD that such α'-martensite of irradiation" was predominantly located inside the (101) oriented grains and had the same orientation itself. The ε-martensite was located inside the (111) oriented grains. The distinctive feature of the α'-phase (bcc) was its extremely fine dispersion (less than 100 nm), along with the presence of many formations with a very large size. The bombardment of the previously deformed 12Cr18Ni10Ti and Cr15Mn14 austenitic steel specimens with 50 keV WC^+ ions leads to a noticeable change in their magnetization, which is related to the formation of the so called "elastic α'-martensite of deformation" the content of which changed as a result of unloading and consecutive loading of the plastically deformed steel specimen. At the same time, different tendencies of the steels to the γ→α' transformation in the given materials govern a larger increase of the α' phase content in the manganese steel in comparison to the chrome-nickel steel. The manifestation of the effect of the "elastic martensite" after irradiation by WC^+ ions increases noticeably, which can be determined not only by the increase in the α' phase content in the specimens, but also by the increase in the internal stresses in the near-surface layer containing the martensite. An increase in the content of α' phase is, in turn, responsible for the additional strengthening (besides the radiation strengthening) of the near-surface layers of the material, in which crack formation can occur with further plastic deformation. Crack formation is dangerous in that the corrosive processes in such areas will be accelerated.

Thus, chrome-nickel steels of 12Cr18Ni10Ti type show better resistance to irradiation with the heavy WC^+ ions in comparison with manganese steel of Cr15Mn14 type, as less martensite of irradiation forms in them.

REFERENCES

1. **Hashimoto, N.** Deformation Mechanisms in 316 Stainless Steel Irradiated at 60 ºC and 330 ºC *Journal of Nuclear Materials* 83 (287) 2000: pp. 538 – 534.
2. **Maksimkin, O. P., et al.** Martensitic Transformations during Deformation and Annealing of the 12Cr18Ni10Ti and 08Cr16Ni11M3 Stainless Steels, Irradiated in BN-350 Reactor *Proceeding of the National Academy of Sciences RK* 5 2005: pp. 145 – 152.
3. **Bogachev, I. N.** Special Features of the Plastic Deformation of Manganese and Nickel Austenitic Alloys *Journal of Physics of Metals and Metallurgy* 16 (4) 1963: pp. 596 – 602.
4. **Johnson, E.** Ion Implantation and Martensitic Transformation in a 17/7 Stainless Steel *Journal of Nuclear Instruments and Methods. In: Physics Research B* 7/8 1985: pp. 212 – 218.
5. **Maksimkin, O. P.** The Defect Structure of the 12Cr18Ni10Ti Steel Irradiated with the Pulse Electron Fluxes and Deformed *Journal of Physics of Metals and Metallurgy* 97 (4) 2004: pp. 1 – 7.
6. **Tsay, K. V., Maksimkin, O. P., Gussev, M. N.** Specific Nature of Microcrystalline Structure Formation at Plastic Deformation in Neutron-Irradiated 12Cr18Ni10Ti Stainless Steel. Bulletin of the National Nuclear Center RK Issue 4 2009: pp. 77 – 86.
7. **Maksimkin, O. P., Berdaliev, D. T.** The Influence of the Reactor Irradiation on the Patterns of the Martensitic γ→α′ Transformation in the 12Cr18Ni10Ti Steel during Deformation. Bulletin of the National Nuclear Center RK Issue 3 2009: pp. 167 – 172.
8. **Gey, N., Petit, B., Humbert, M.** Electron Backscattered Diffraction Study of ε/α′-martensitic Variants Induced by Plastic Deformation in 304 Stainless Steel *Metallurgical Transaction A* 36 2005: pp. 3291 – 3299.
9. **Pan, X., Wu, X., Stubins, J.** Analysis of Notch Strengthening of 316L Stainless Steel with and without Irradiation-induced Hardening Using EBSD and FEM *Journal of Nuclear Material* 361 2007: pp. 228 – 238. http://dx.doi.org/10.1016/j.jnucmat.2006.12.033
10. **Maksimkin, O. P., Tsai, K. V.** Magnetometric Study of the Distinctive Features of the Martensitic γ→α′ Transformation in the Neutron Irradiated 12Cr18Ni10Ti Steel *Metals* 5 2008: pp. 39 – 47.